13th World Conference on Earthquake Engineering
Vancouver, B.C., Canada
August 1-6, 2004
Paper No. 3369

NONLINEAR EXPERIMENTAL RESPONSE OF PRIMARY-SECONDARY SYSTEMS UNDER REPEATED SEISMIC EXCITATION

H.H. MOHAMMED[1], T.S. AZIZ[2], A. GHOBARAH[2]

SUMMARY

Repeated ground motion was observed in several recent earthquakes in California, Taiwan, Romania, Turkey and Japan. In these earthquakes the main structure or Primary system (P-system) may remain undamaged on the first or second excitation in the seismic sequence, yet exhibit a nonlinear response on further excitations. It is important to study the response of the supported non-structural equipment in such events. Non-structural components or Secondary systems (S-system) are crucial for the functioning of lifeline facilities such as hospitals and power plants. The most critical case of concern of the coupled Primary-Secondary system (PS-system) is the near tuned case; causing quasi-resonance. Detuned response can be of concern in cases where at least one of the two subsystems yields in the seismic event. In previous analytical and experimental studies on coupled PS-system linear and nonlinear response; little or no concern was given to the effect of torsional coupling as a result of P-system stiffness eccentricity, mass eccentricity of the P-system or S-system location eccentricity relative to the Centre of Mass (CM) of the P-system. These parameters are present in most real structures due to functionality requirements and space optimization. In this shake-table research program, the nonlinear torsionally coupled PS-system response is characterized. The research program also serves as a means of calibrating the analytical solution of the transient response. The PS-system model is excited by a synthetic seismic sequence. The P-system and S-system are modeled as lumped masses. P-system eccentricity is induced through static or dynamic coupling; whereas S-system eccentricity is induced through varying the location of attachment relative to the P-system CM. Torsional interaction and response amplification of the coupled PS-system are characterized and quantified. Experimental findings show that the torsional yielding of the primary system has significant implications on the de-amplification of near tuned secondary system response. The location of the S-system affects its peak response amplification. A detailed analytical model is developed to simulate the experimental behavior.

[1] PhD. Candidate, Dept. of Civil Engineering, McMaster University, Canada, mohammhh@mcmaster.ca
[2] Professor, Dept. of Civil Engineering, McMaster University, Canada

INTRODUCTION

Recently a number of earthquake events have been characterized by the occurrence of seismic sequences in California, Taiwan, Romania, Turkey and Japan (Amadio et. al. [1], Decannini et. al. [2], Elnashai et. al. [3]). Under such circumstances both structural and nonstructural components will have to sustain multiple earthquake ground motions. Some investigations have already addressed the effect of this phenomenon on the nonlinear response of Single Degree of Freedom (SDOF) systems (Muria Vila et. al. [4]) typically used for the representation of the structure or Primary system (P-system). However investigations into the coupled response of structural and nonstructural components or Secondary systems (S-system) under repeated seismic excitation is scarce. At the same time the investment distribution outlined by Figure 1 indicates that greater attention should be paid also to the effect of such events on the response of non structural components.

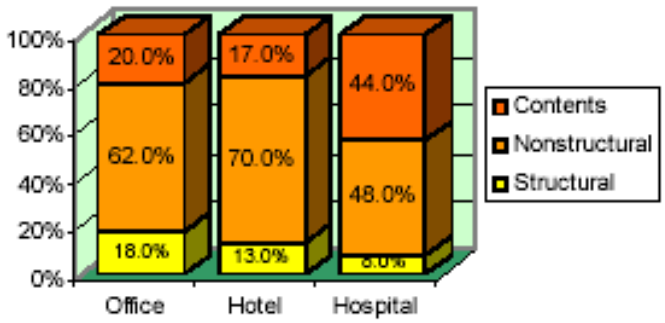

Figure 1 Typical Investment in Building Construction
(Whittiker & Soong [5] after E. Miranda)

Segal and Hall [6] conducted an experimental investigation on the nonlinear translational response of appendages mounted on yielding primary structures using small-scale shake table experiments. Adam [7] conducted small-scale experiments on translational behaviour of a S-system supported on a yielding Multi-Degree of Freedom (MDOF) P-systems. Villaverde [8] indicated that research is needed to study the influence of the torsional motion of a supporting structure on the response of attached secondary elements. In this investigation the experimental response of torsionally coupled nonlinear PS-systems is characterized. The effect of the S-system eccentricity with respect to the P-system's Centre of Mass (CM) and Centre of Rigidity (CR) had not been sufficiently investigated experimentally. In addition an analytical model is developed using the modified Bouc-Wen-Baber-Noori (modified BWBN) that is capable of simulating the nonlinear behavior of the torsionally coupled PS-system.

EXPERIMENTAL MODEL AND TEST SETUP

Torsionally Coupled PS-system Model

The modeled P-system in this shake table investigation was comprised of a square aluminum platform (300mm x 300 mm) upon which additional mass is attached in the form of 30 mm long steel strips. The platform was supported by circular aluminum rods of diameter 3 mm and varied lengths for stiffness adjustment. Up to three aluminum rods could be clamped at each of the four corners of the P-system platform permitting for a variety of static coupling cases. Since the shake table excitation was unidirectional only one axis of asymmetry is considered in this investigation. The S-system mass representing 3.2% of the P-system mass can be attached at various locations to investigate the effect of S-system position eccentricity on the PS-system response. The S-system is supported by two thin rectangular

aluminum strips. The uncoupled translational frequencies of both subsystems are near tuned to achieve a target frequency of 10 Hz. Near tuning is the most critical case for elastically responding PS-systems resulting in the quasi-resonance case. Figure 2 illustrates details of the Shake table platform, the P-system model with stiffness eccentricity and the locations 1 to 5 where the S-system is attachable for position eccentricity of the equipment. Table 1 lists 25 cases considered incorporating static coupling through stiffness eccentricity of the P-system and position eccentricity of the S-system. The number of supports on the left side and right side refer to the side view of Figure 2 to achieve the desired level of stiffness eccentricity. Table 2 lists the achievable translational frequency and corresponding rotational frequency as well as the frequency ratio (ω_θ / ω), where ω is the translational angular frequency and ω_θ is the rotational angular frequency for the P-system. For the stiffness eccentric cases, the Center of Mass (CM) coincides with the geometric center of the P-system platform whereas the Center of Rigidity (CR) assumes different locations depending on initial eccentricity listed in Table 1 and later yielding of the P-system. An accelerometer capable of measuring within (±5g) was attached to each of the subsystems. A third accelerometer was attached to the shake table to measure the base acceleration. The range of stiffness eccentricities "e" considered was from 0 % to 24.54 % for the P-system. The range of position eccentricities "e" considered was from 0 % to ±37.74 % for the attached S-system.

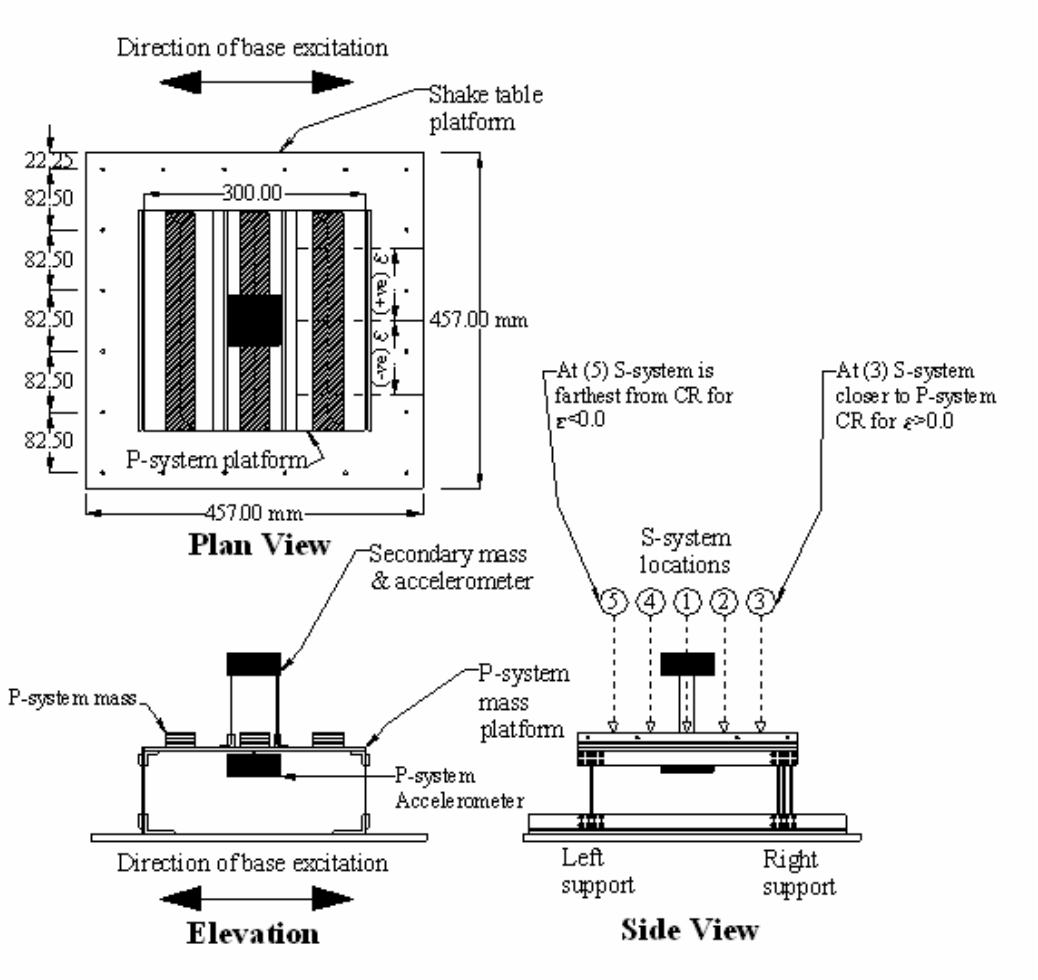

Figure 2 Stiffness eccentric experimental model details

Table 1 Stiffness eccentric experiments for coupled PS-system

Experiment No.	No. of supports		P-system C.R. stiffness eccentricity "e" (%)	S-system location eccentricity "ε" (%)
	Left end	Right end		
1	2	2	0.00	0.00
2	2	3	9.81	0.00
3	2	4	16.36	0.00
4	2	5	21.03	0.00
5	2	6	24.54	0.00
6	2	2	0.00	18.87
7	2	3	9.81	18.87
8	2	4	16.36	18.87
9	2	5	21.03	18.87
10	2	6	24.54	18.87
11	2	2	0.00	37.74
12	2	3	9.81	37.74
13	2	4	16.36	37.74
14	2	5	21.03	37.74
15	2	6	24.54	37.74
16	2	2	0.00	-18.87
17	2	3	9.81	-18.87
18	2	4	16.36	-18.87
19	2	5	21.03	-18.87
20	2	6	24.54	-18.87
21	2	2	0.00	-37.74
22	2	3	9.81	-37.74
23	2	4	16.36	-37.74
24	2	5	21.03	-37.74
25	2	6	24.54	-37.74

Table 2 P-system frequencies for studied cases of a stiffness eccentric system

No. of supports		Support length (mm)	Fundamental frequency (Hz)	Torsional frequency (Hz)	Error %	Stiffness eccentricity "e" %	$\frac{\omega_\theta}{\omega}$
Left end	Right end						
2	2	67	9.67	13.03	3.26	0.00	1.35
2	3	70	9.74	14.19	2.55	9.81	1.46
2	4	72	9.70	15.72	2.96	16.36	1.62
2	5	73	9.83	17.38	1.70	21.03	1.77
2	6	75	9.75	18.47	2.47	24.54	1.89

The effect of mass eccentricity of the P-system was also considered in this investigation. Figure 3 illustrates the positioning of eccentric mass strips on the side of the P-system platform. The desired level of dynamic coupling is thus controlled by the number of displaced steel strips from the central position to

the side of the P-system platform. The total mass affecting the translational inertia was maintained the same however; such that the translational frequency remains around 10 Hz. The considered range of mass eccentricity was from 0% to 10.87% as the maximum achievable mass eccentricity by the model was ±11 %.

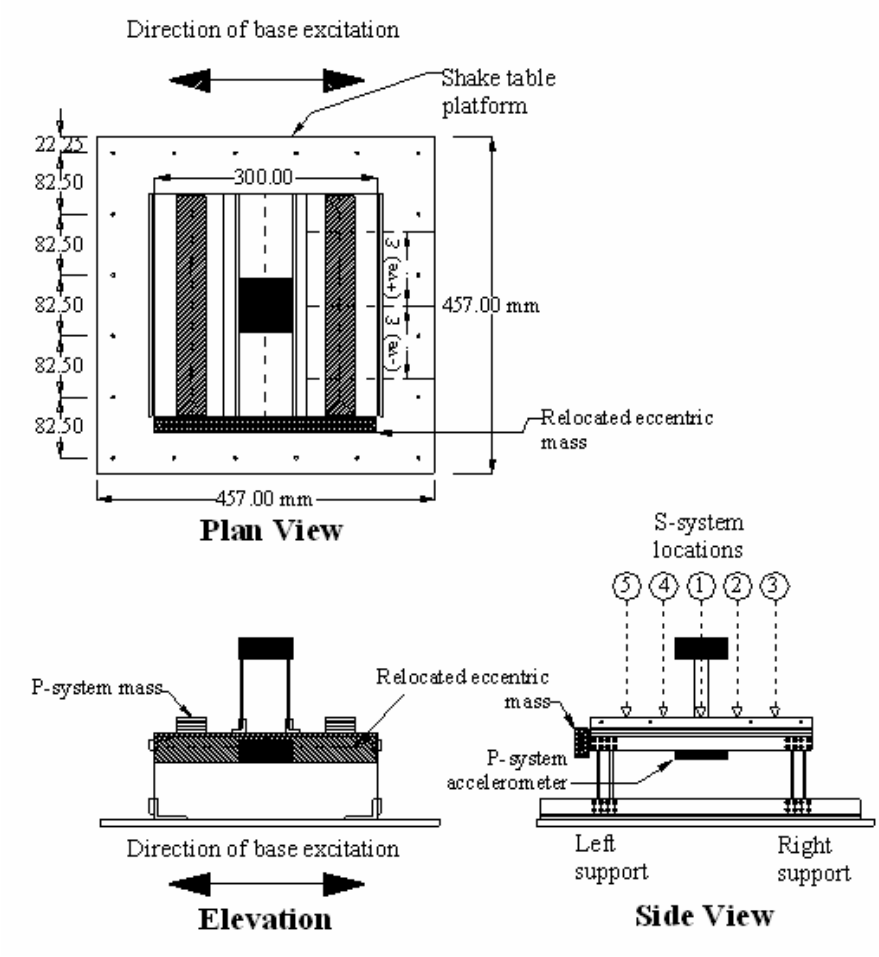

Figure 3 Mass eccentric experimental model details

The level of P-system eccentricity "e" whether mass eccentricity or stiffness eccentricity was calculated by equation (1), where the distance between the CM and CR represents the initial pre-yield eccentricity.

$$e = \frac{Dist.\ \ between\ \ CM\ \ \ and\ \ \ CR}{Dist.\ \ between\ \ \ corner\ \ \ columns} \times 100 \qquad (1)$$

For the considered cases of mass eccentricity in Table 3 it is noted that the number of supports on the left end and right end where kept the same so that no static coupling is developed. Table 4 lists the supports' free lengths in mm, the achievable translational frequency and corresponding rotational frequency in Hz for the mass eccentric P-system. Additionally the frequency ratio for each of the mass eccentric cases (ω_θ / ω) is evaluated for the pre-yield condition.

Table 3 Mass eccentric experiments for coupled PS-system

Experiment No.	No. of supports		P-system C.M. mass eccentricity "e" (%)	S-system location eccentricity "ε" (%)
	Left end	Right end		
1	4	4	0.00	0.00
2	4	4	-2.72	0.00
3	4	4	-5.43	0.00
4	4	4	-8.13	0.00
5	4	4	-10.87	0.00
6	4	4	0.00	18.87
7	4	4	-2.72	18.87
8	4	4	-5.43	18.87
9	4	4	-8.13	18.87
10	4	4	-10.87	18.87
11	4	4	0.00	37.74
12	4	4	-2.72	37.74
13	4	4	-5.43	37.74
14	4	4	-8.13	37.74
15	4	4	-10.87	37.74
16	4	4	0.00	-18.87
17	4	4	-2.72	-18.87
18	4	4	-5.43	-18.87
19	4	4	-8.13	-18.87
20	4	4	-10.87	-18.87
21	4	4	0.00	-37.74
22	4	4	-2.72	-37.74
23	4	4	-5.43	-37.74
24	4	4	-8.13	-37.74
25	4	4	-10.87	-37.74

Table 4 P-system frequencies for studied cases of a mass eccentric system

No. of supports		Support length (mm)	Fundamental frequency (Hz)	Torsional frequency (Hz)	Error %	Mass eccentricity "e" %	$\frac{\omega_\theta}{\omega}$
Left end	Right end						
4	4	85	9.75	13.19	2.54	0.00	1.35
4	4	85	9.78	12.52	2.24	-2.72	1.28
4	4	85	9.73	12.05	2.73	-5.43	1.24
4	4	85	9.72	12.01	2.83	-8.13	1.24
4	4	85	9.71	12.35	2.92	-10.87	1.27

Figure 4 illustrates a view of the assembled PS-system model mounted on the unidirectional shake table with the S-system eccentrically positioned. P-system support elements damaged by yielding were replaced after every experiment.

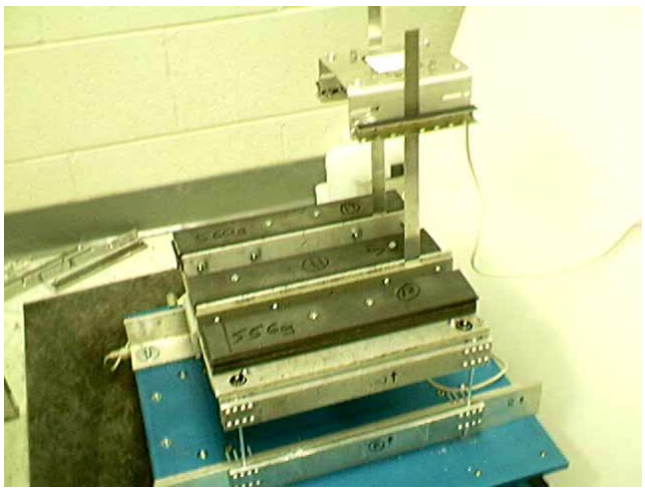

Figure 4 PS-system model

Repeated Base Excitation

A synthetically generated base excitation placing continuous demand on the modeled PS-system was desired for this investigation rather than the use of scaled earthquake records; as scaling may typically distort the frequency content of the original earthquake record. It was important to maintain the frequency content of the non-stationary signal intact without violating the stroke limitations of the shake table at ±76 mm. The Kanai-Tajimi Power Spectral Density Function (PSDF) was used to this end employing soil parameters characteristic of rock soil conditions following Elgadamsi et. al. [9]. The base excitation peak acceleration was 0.94g which is characteristic of severe earthquakes that may affect certain stiff structures of industrial facilities typically designed to behave elastically in a seismic event. The base excitation is applied to the modeled PS-system repeatedly as illustrated in Figure 5 until yielding and eventually collapse of the P-system is achieved. The response of the attached S-system remains elastic throughout all tests.

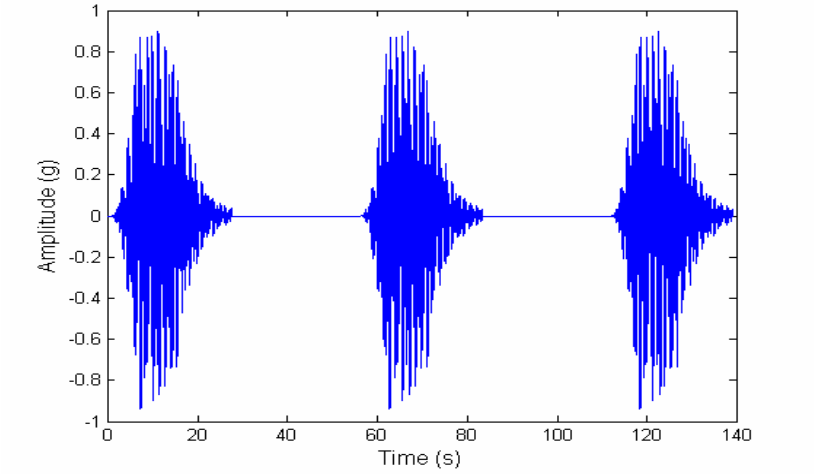

Figure 5 Repeated base excitation

Figure 6 illustrates a comparison between the generated synthetic record's elastic response spectrum as compared to the elastic response spectrum of the 1971 San Fernando Earthquake at 1.6% damping which represents the experimentally measured damping of the modeled P-system by the half power band width

method. Damping of the uncoupled S-system was evaluated experimentally to be at 0.15%. It is noted that both spectra exhibit similar characteristics within the frequency range of interest with respect to the pre and post yield modal frequencies of the coupled PS-system.

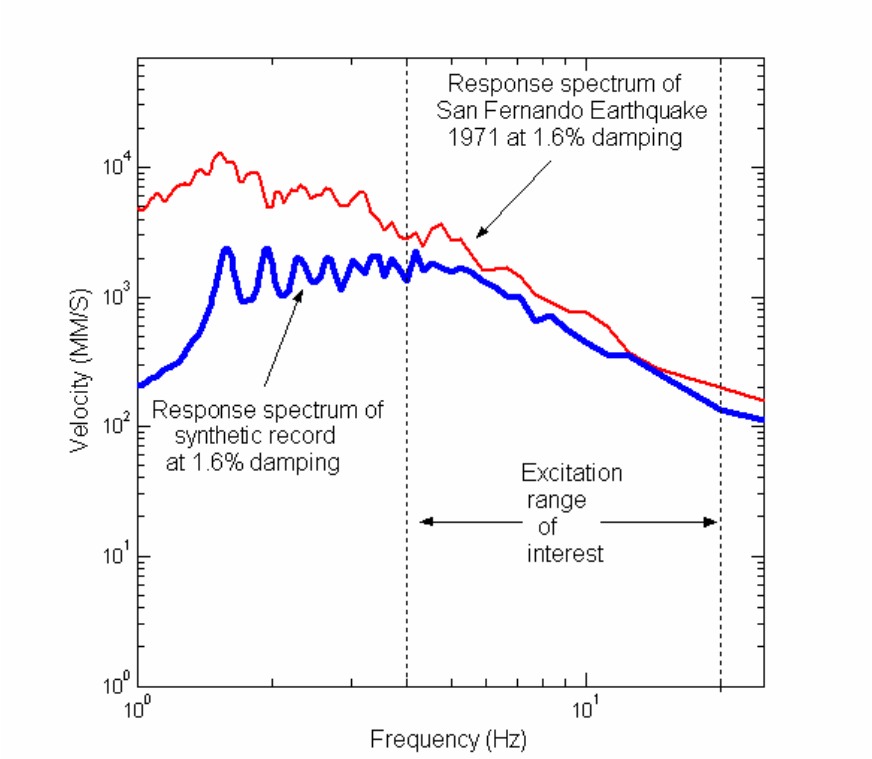

Figure 6 Response spectrum for generated record

EXPERIMENTAL RESULTS AND DISCUSSION

Peak acceleration response

The peak acceleration response of each test run for each experiment in Table 1 and Table 3 is extracted from the time history responses of the coupled PS-system and plotted for comparison. Figure 7 and Figure 8 illustrate the peak acceleration responses of the stiffness eccentric and mass eccentric PS-systems respectively. In each of the figures "e" stands for the P-system eccentricity, and "ep" stands for "e"; the location eccentricity of the attached S-system. The black bars represent the peak command signal to the shake-table at 0.94g, the dark grey bars represent the peak base excitation as recorded by the shake-table accelerometer, the light grey bars represent the coupled P-system peak acceleration response and the white bars represent the coupled S-system peak acceleration response. It is observed from Figure 7 and Figure 8 that the response of the near tuned S-system is amplified substantially relative to the corresponding P-system response peak. For PS-systems surviving more than 2 test runs it is noted that initially the peak S-system acceleration is more than twice that of the corresponding P-system acceleration. With successive excitation of the PS-system, the P-system yields and detuning results due to the drop in P-system's fundamental frequency. Yielding of the P-system occurs as a result of the formation of plastic hinges at the ends of the fixed end supports. For the stiffness eccentric experiments the left side supports are always set to be weaker than the right side as illustrated in Figure 2 and therefore they yield first as expected.

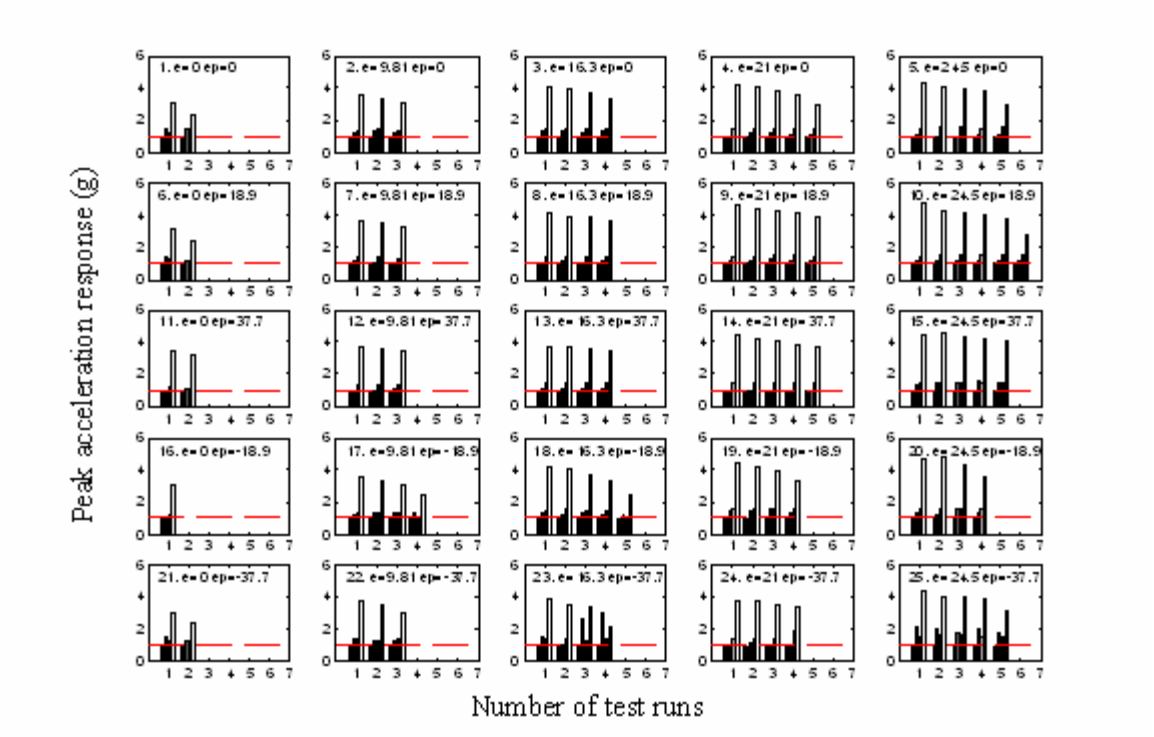

Figure 7 Stiffness eccentric coupled PS-system peak responses (g's)

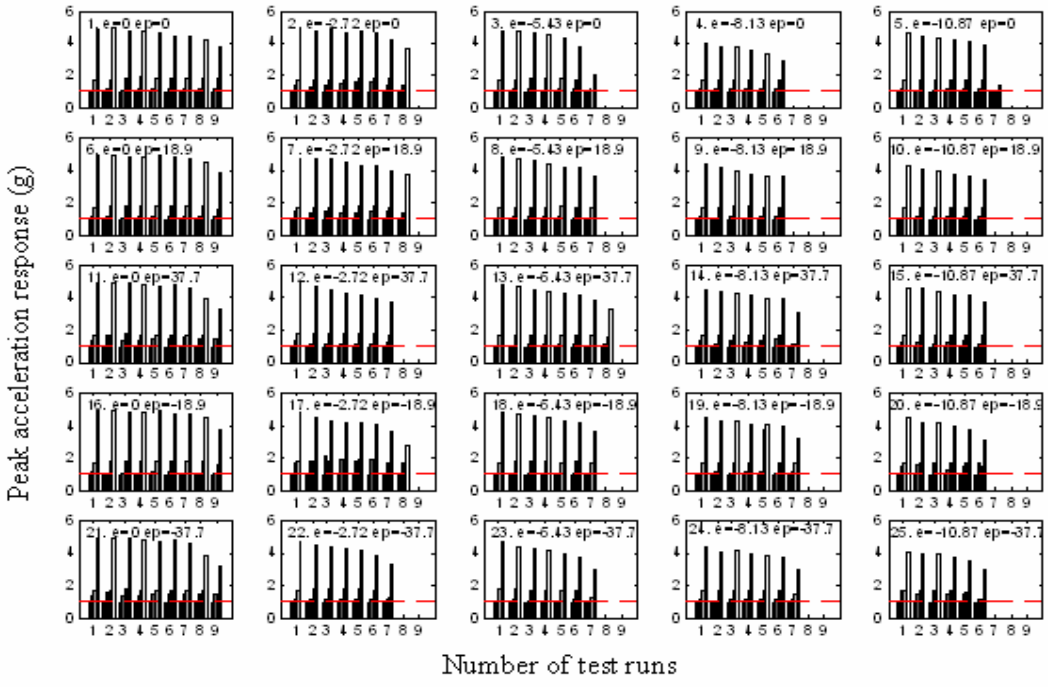

Figure 8 Mass eccentric coupled PS-system peak responses (g's)

Although in all tests the fundamental frequency was maintained as much as possible close to 10Hz, the torsional frequency changed as shown in Table 2 and Table 4. For a stiffness eccentric P-system the ratio (ω_θ / ω) increased with more static coupling, which increased the structure's stiffness in torsion. In addition this meant that the torsional mode was excited by a smaller amplification from the generated record as shown in Figure 6. This explains why the stiff PS-system models exhibiting greater static coupling were able to sustain more test runs as shown in Figure 7. This experimental observation concurs with conclusions of Kan and Chopra [10] based on the numerical modeling of simple torsionally coupled inelastic systems; that for buildings strong in torsion yielding is essentially governed by the building's yield strength in translation. Greater P-system strength in torsion has resulted in greater amplification of the S-system response for the same case of S-system location eccentricity. On the other hand, for the mass eccentric tests; the ratio (ω_θ / ω) decreased with the increase in dynamic coupling. This meant that the torsional mode was excited by a greater amplification as seen from Figure 6. Therefore greater dynamic coupling resulted in quicker yielding and a decrease in the number of test runs as seen from Figure 8. Figure 8 also indicates that with greater dynamic coupling of the P-system as a result of the mass eccentricity there is a reduction in the peak S-system response acceleration for the same case of S-system position eccentricity. The phenomena is most apparent when comparing experiments 21 to 25 in Figure 8.

ANALYTICAL MODELING

The experimentally modeled PS-system was observed to exhibit both material and geometric nonlinearity upon yielding of the P-system, it was important therefore to adopt a numerical formulation capable of representing this combined behavior. One of the most widely used and versatile mathematical models that currently exists is the modified Bouc-Wen-Baber-Noori model (modified BWBN), Wen [11],Baber and Noori, [12], Baber and Noori [13], Foliente [14]. This is a smooth varying hysteretic model. For a Single Degree of Freedom system (SDOF) exhibiting nonlinear behavior, the stiffness component of the total restoring force f_S is represented as in equation (2).

$$f_s(r(t), z(t), t) = f_E + f_H = \alpha k r(t) + (1-\alpha) k z(t) \tag{2}$$

Where f_E is the elastic portion of the stiffness restoring force, f_H is the hysteretic portion of the stiffness restoring force, k is the initial pre-yield stiffness of the supporting element, α is the post yield to pre-yield stiffness ratio, $r(t)$ is the relative deformation, $z(t)$ is the hysteretic parameter. The resulting equation of motion for the SDOF system becomes

$$m\ddot{r}(t) + c\dot{r}(t) + \alpha k r(t) + (1-\alpha) k z(t) = f(t) \tag{3}$$

Where m is the mass and c is the damping. The hysteretic parameter $z(t)$ is generally governed by the first order ordinary differential equation (1st ODE) in the derivative of z as follows,

$$\dot{z}(t) = h(z)\left\{ \frac{A\dot{r}(t) - \nu(\beta\left|\dot{r}(t)\right\|z(t)\right|^{n-1} z(t) + \gamma\dot{r}(t)\left|z\right|^{n})}{\eta} \right\} \tag{4}$$

Where A, β, γ, n are hysteretic loop shape parameters, ν is a strength degradation parameter, η is a stiffness degradation parameter, $h(z)$: is a function that governs the hysteretic loop pinching behavior. As the dynamic system undergoes inelastic deformation, hysteretic energy is dissipated. The parameters controlling stiffness and strength degradation may therefore be altered during the dynamic analysis as functions of the dissipated hysteretic energy ε_h.

$$\varepsilon_h = \int f_H \, du \tag{5}$$

The strength degradation parameter as a function of hysteretic energy is:

$$\nu(\varepsilon_h) = 1.0 + \delta_\nu \varepsilon_h \tag{6}$$

The stiffness degradation parameter as a function of the hysteretic energy is:

$$\eta(\varepsilon_h) = 1.0 + \delta_\eta \varepsilon_h \tag{7}$$

Where δ_v determines the rate of strength degradation and δ_η determines the rate of stiffness degradation. The maximum achievable value for the *z(t)* parameter is obtained by equation (8).

$$z_u = \left[\frac{A}{\nu(\beta+\gamma)}\right]^{\frac{1}{n}} \tag{8}$$

Further details regarding the pinching or slip formulation used can be found in Foliente [14]. In the case of a torsionally coupled PS-system, deformations in the two horizontal perpendicular directions are coupled. Equations (9) and (10) introduced by Wang and Wen [15] as a generalization of the original formulation by Park et. al. [15] for biaxial hysteretic response, were used here for the torsionally coupled PS-system supports. The pinching function *h(z)* was also implemented for the biaxial hysteretic formulation for completeness; though not needed in the current investigation for comparison with the experimental results.

$$\dot{z}_x(t) = \frac{h(z)}{\eta}\left\{A\dot{r}_x - \nu z_x\{|\dot{r}_x||z_x|^{n-1}(\beta+\gamma\,\mathrm{sgn}(\dot{r}_x z_x)) + \left(\frac{U_x^{\,y}}{U_y^{\,y}}\right)|\dot{r}_y||z_y|^{n-1}(\beta+\gamma\,\mathrm{sgn}(\dot{r}_y z_y))\}\right\} \tag{9}$$

$$\dot{z}_y(t) = \frac{h(z)}{\eta}\left\{A\left(\frac{U_x^{\,y}}{U_y^{\,y}}\right)\dot{r}_y - \nu z_y\{|\dot{r}_x||z_x|^{n-1}(\beta+\gamma\,\mathrm{sgn}(\dot{r}_x z_x)) + \left(\frac{U_x^{\,y}}{U_y^{\,y}}\right)|\dot{r}_y||z_y|^{n-1}(\beta+\gamma\,\mathrm{sgn}(\dot{r}_y z_y))\}\right\} \tag{10}$$

Where $U_x^{\,y}$ and $U_y^{\,y}$ are the yield displacements of a support element in the two horizontal perpendicular directions x and y respectively.

Solution Approach

To solve the coupled nonlinear 2nd order MDOF system equation of motion, it is first rewritten in form of a 1st order state-space equation (11).

$$\begin{Bmatrix}\dot{u}(t)\\ \ddot{u}(t)\\ \dot{z}(t)\end{Bmatrix} = \begin{bmatrix}0 & I & 0\\ -M^{-1}K_E & -M^{-1}C & -M^{-1}K_H\\ 0 & \left[\frac{dz}{du}\right] & 0\end{bmatrix}\begin{Bmatrix}u(t)\\ \dot{u}(t)\\ z(t)\end{Bmatrix} + \begin{bmatrix}0\\ M^{-1}\\ 0\end{bmatrix}F_g(t) \tag{11}$$

In equation (11); *M* is the PS-system mass matrix, *C* is the damping matrix, K_E is the elastic stiffness component matrix, K_H is the hysteretic stiffness component matrix, *I* is the identity matrix, *0* is a zero matrix, [*dz/du*] is the matrix of derivatives of the hysteretic parameter z as a function of system lumped degrees of freedom {u}; that is formulated for the torsionally coupled system. The form of equation (11) is adopted from Barroso et al. [17] and To [18] with modifications to incorporate equations (9) and (10). Equation (11) is typically simplified to the state-equation form in equation (12).

$$\dot{q}(t) = A_{dyn}q(t) + F \tag{12}$$

Where *q(t)* is the state vector including all variables in the 1st order ODE, A_{dyn} is the dynamical matrix including the mass, stiffness and damping matrices and *F* is the external ground excitation .

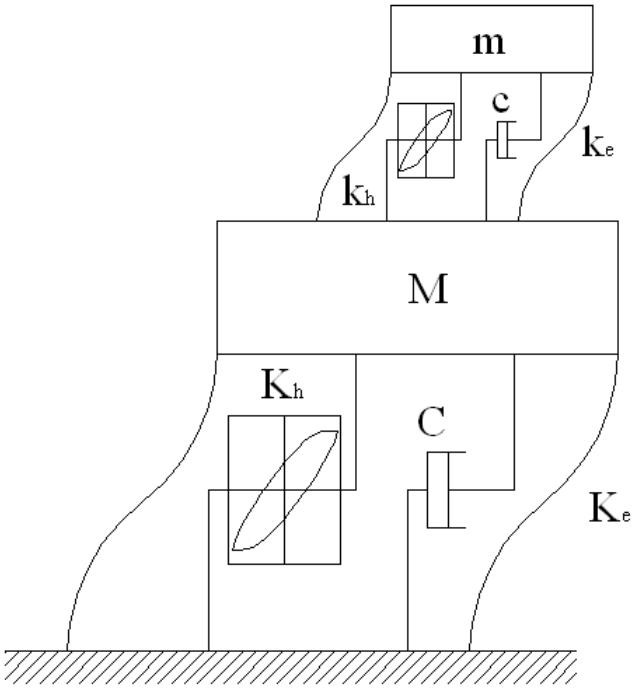

Figure 9 Analytical model of the coupled nonlinear PS-system

Figure 9 illustrates a side view schematic of the analytical nonlinear model developed for the torsionally coupled PS-system. In Figure 9, M refers to the P-system mass and m refers to the S-system mass, K_h refers to the P-system hysteretic stiffness component and k_h refers to the S-system hysteretic stiffness component, C refers to the P-system damping and c refers to the S-system damping, whist K_e refers to the P-system elastic stiffness component and k_e refers to the S-system elastic stiffness component. A multitude of numerical methods can be used at this point to solve the 1st order ODE including the efficient variable order solvers based on the Numerical Differentiation Formulas (NDFs) incorporated in the MATLAB. A MATLAB code was developed using the formulation outlined above for the simulation of the torsionally coupled PS-system linear and nonlinear response. Geometric nonlinearities were also considered for large rotations and P-Δ effects. Although for comparison purposes with the experimental program only one excitation component is needed, the developed code can handle dual perpendicular base excitations and the corresponding rotational excitation as well.

ANALYTICAL RESULTS COMPARISON

To demonstrate the efficiency of the developed model in simulating the behavior of the PS-system, the dissipated energy from each of the coupled subsystems is evaluated for experiment 1 in Table 1 using the experimental response data and the analytical response data. The model hysteretic loop shape parameters A, β and γ are evaluated as functions of the material properties using plastic section analysis of the supporting elements. In evaluating the dissipated energy which represents the hysteretic and damping energies, the area enclosed by the force deformation plot for each subsystem is evaluated for experimental and analytical response.

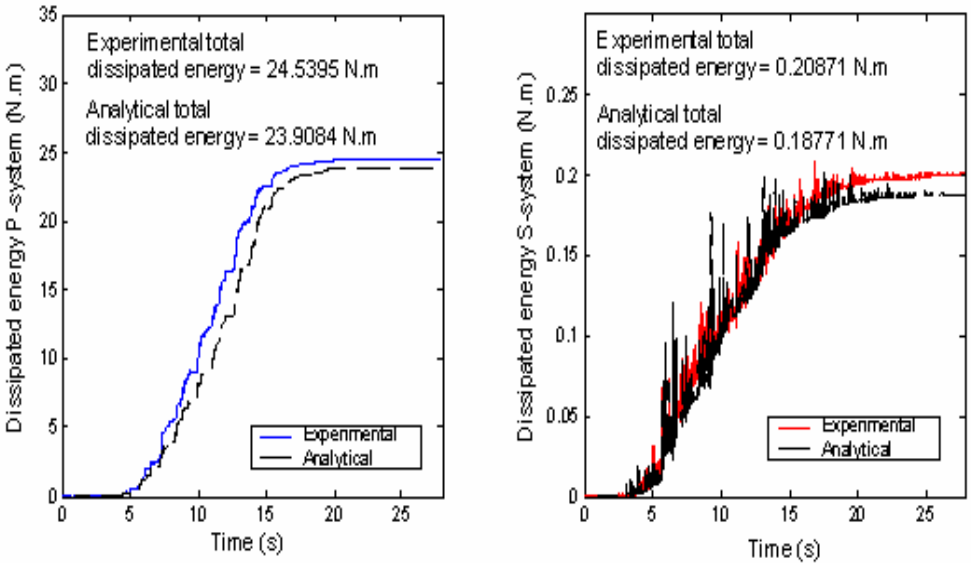

Figure 10 Dissipated energy comparison for stiffness eccentric experiment 1, 1st run

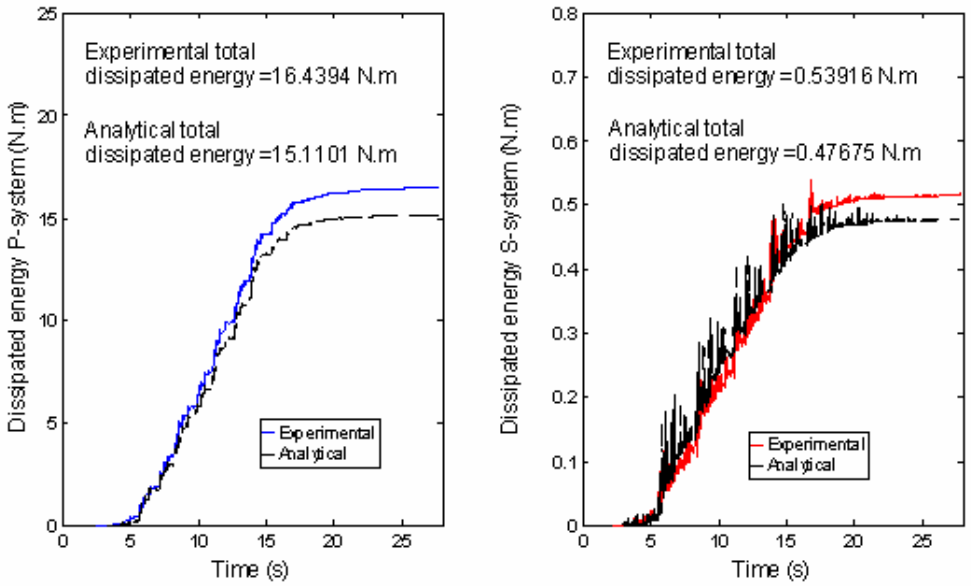

Figure 11 Dissipated energy comparison for stiffness eccentric experiment 5, 1st run

Figure 10 and Figure 11 demonstrate that the analytically evaluated dissipated energy for each of the coupled subsystems is in favorable agreement with dissipated energy obtained using the experimental response data indicating that the analytical model is capable of simulating the nonlinear dynamic behavior of the coupled PS-system. Figure 12 illustrates a comparison of the experimental versus analytical dynamic restoring-force deformation response of the P-system at the CM which also shows good agreement.

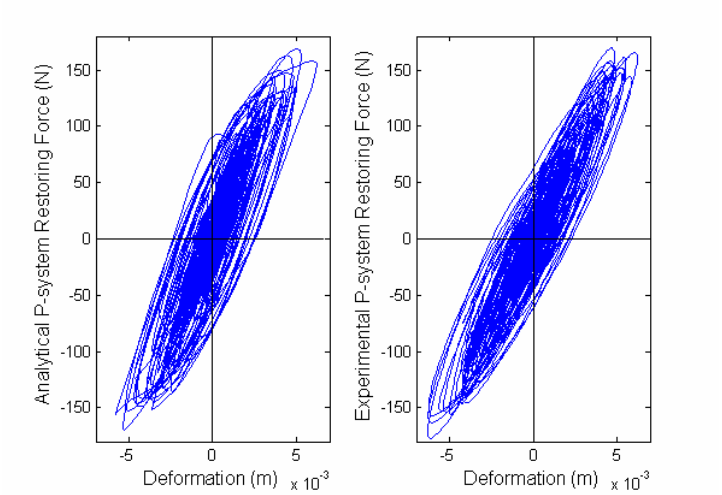

Figure 12 P-system force deformation response comparison for stiffness eccentric experiment 5, 1st run

CONCLUSIONS

A new small scale experimental model was implemented to study the behavior of torionally coupled PS-systems under repeated seismic excitation. The experimental program was beneficial in identifying the behavior of near tuned; torsionally coupled PS-systems with the P-system exhibiting nonlinear response.

1. For the studied cases; where the mass ratio between the S-system and the P-system is maintained at 3.2%, it was observed that the S-system response is greatly amplified in the near tuned case in all the tests. The S-system amplification reduced with successive yielding of the P-system which resulted in the softening of the P-system and subsequent detuning of both subsystems. In all experiments the S-system remained elastic.
2. At an uncoupled frequency of 10 Hz, and with (ω_θ / ω)>1.3 for all stiffness eccentric cases the P-system was torsionally stiff, accordingly its yield strength in translation predominantly controlled the number of test runs it could sustain prior to failure; which appeared to increase as more supports with greater length were added to increase the static torsional coupling whilst maintaining the fundamental frequency as close to 10 Hz as possible. Additionally as the ratio (ω_θ / ω) increased with greater static torsional coupling the torsional mode was excited by a smaller amplification on the response spectrum of the synthetically generated record. These conditions combined have contributed to the survival of the P-system through more test runs with increased static coupling.
3. For the mass eccentric experiments the ratio (ω_θ / ω) decreased with increased dynamic coupling meaning that the torsional mode received greater amplification on the response spectrum of the synthetically generated record. In all the mass eccentric experiments there was no static coupling and hence the number and length of supports was unchanged, therefore the translational yield strength under static conditions was unchanged. Increased dynamic torsional coupling induced a torsional moment that resulted in the shorter life of the P-system in terms of test runs.
4. Greater dynamic torsional coupling of the P-system has generally resulted in reduced amplification of the attached S-system for the same case of S-system location eccentricity.
5. A model incorporating both material and geometric nonlinearities was implemented in a MATLAB code utilizing the biaxial modified BWBN formulation that is capable of simulating the experimental torsionally coupled PS-system model as well as a variety of other systems exhibiting various levels of nonlinear response. The analytically calculated energy dissipation was compared to the experimentally obtained energy dissipation of both subsystems and favorable agreement was achieved.

REFERENCES

1. Amadio C., Fragiacomo M., Rajgelj S., "*The effect of Repeated Earthquake Ground Motions on the Non-linear Response of SDOF systems*", Earthquake Engng. & Structural Dyn., 2003, 32, pp. 291-308
2. Decanini L., Gavarini C., Mollaioli F., "*Some remarks on the Umbria-Marchr earthquake of 1997*," European Earthquake Engineering, 2000, Vol 3, pp. 18-48.
3. Elnashai A. S., Bommer J. J., Martinez-Periera A., "*Engineering implications of strong-motion records from recent earthquakes*," 11th European Conference on Earthquake Engineering, ed. by Bisch P., Labbé P. & Pecker A.(eds.), Paris, France 1998, CD-ROM
4. Muria Vila D., Toro Jaramillo A. M., "*Effects of several events recorded at a building founded on soft soil*," 11th European Conference on Earthquake Engineering; ed. by Bisch P., Labbé P. & Pecker A.(eds.), Paris, France 1998, CD-ROM
5. Whittaker, A. S., Soong, T. T., " *An Overview of Nonstructural Component Research at Three U.S. Earthquake Engineering Research Centers*," Proceedings of Seminar on Seismic Design, Performance and Retrofit of Nonstructural Components in Critical Facilities, ATC-29-2, Session V: Risk and Performance Evaluation I, 2003, pp.271-280.
6. Segal D., Hall W.J., "*Experimental Seismic Investigation of Appendages in Structures*", Civil Engineering Studies, Structural Research Series No. 545, University of Illinois: Urbana, IL, 1989.
7. Adam C. "*Dynamics of Elastic-plastic Shear frames with Secondary Structures: Shake Table and Numerical Studies*", Earthquake Engng. & Structural Dyn., 2001, 30, pp. 257-277.
8. Villaverde, R. "*Seismic Design of Secondary Structures: State of the Art*", Journal of Structural Engineering, 1997, Vol. 123, No. 8, pp.1011-1019.
9. Elgadamsi, F. E., Mohraz, B., Lee, C. T., and Moayyad, P., "*Time-Dependent Power Spectral Density of Earthquake Ground Motion*", Int. J. Soil Dynamics and Earthquake Eng., 1988, 7, No. 1, pp. 15-21.
10. Kan, C., and Chopra, A., "*Linear and Nonlinear Earthquake Responses of Simple Torsionally Coupled Systems*," Report No. UCB/EERC-79/03, University of California at Berkeley, 1979.
11. Wen Y.K, "*Equivalent Linearization for Hysteretic Systems Under Random Excitation*," Journal of Applied Mechanics, 1980, Vol. 47, p.150-154.
12. Baber T., and Noori M.N., "*Random Vibration of Degrading Pinching Systems*," Journal of Engineering Mechanics, ASCE, 1985, Vol. 111 (8), p.1010-1026.
13. Baber T., and Noori M.N., "*Modeling General Hysteretic Behavior and Random Vibration Applications*," Journal of Engineering Mechanics, ASCE, 1986, Vol. 107 (EM6), p.1069-1089.
14. Foliente G.C., "*Hysteretic Modeling of Wood Joints and Structural Systems*," Journal of Structural Engineering, 1995, Vol. 121 (6), p.1013-1022.
15. Wang C. H., Wen Y. K., "*Evaluation of Pre-Northridge Low-Rise Steel Buildings I: Modeling*," Journal of Structural Engineerig, 2000, Vol. 126, No. 10, pp.1160-1168.
16. Park Y. J., Wen Y. K., Ang H-S., "*Random Vibration of Hysteretic Systems Under Bi-Directional Ground Motion*," Earthquake Engineering and Structural Dynamics, 1986, Vol. 14, 543-557.
17. Barroso L. R., Breneman S. E. and Smith H. A., "*Evaluating the Effectiveness of Actively Controlled Structures within the Context of Performance-Based Engineering.*" Proceedings 6th National Conference on Earthquake Engineering, Seattle, Washington, paper No. 123, 1998.
18. To C. W. S., "*Nonlinear Random Vibrations, Analytical Techniques and Applications*," Swets & Zeitlinger Publishers, Netherlands, 2000.